chemosensors

MDPI

Review

Gas Sensors Based on Copper Oxide Nanomaterials: A Review

Stephan Steinhauer

Department of Applied Physics, KTH Royal Institute of Technology, SE-106 91 Stockholm, Sweden; ssteinh@kth.se

Abstract: Metal oxide semiconductors have found widespread applications in chemical sensors based on electrical transduction principles, in particular for the detection of a large variety of gaseous analytes, including environmental pollutants and hazardous gases. This review recapitulates the progress in copper oxide nanomaterial-based devices, while discussing decisive factors influencing gas sensing properties and performance. Literature reports on the highly sensitive detection of several target molecules, including volatile organic compounds, hydrogen sulfide, carbon monoxide, carbon dioxide, hydrogen and nitrogen oxide from parts-per-million down to parts-per-billion concentrations are compared. Physico-chemical mechanisms for sensing and transduction are summarized and prospects for future developments are outlined.

Keywords: chemical sensors; gas sensors; nanomaterials; nanoparticles; nanowires; copper oxide; cupric oxide; cuprous oxide; air quality monitoring; volatile organic compounds

Citation: Steinhauer, S. Gas Sensors Based on Copper Oxide Nanomaterials: A Review. *Chemosensors* **2021**, *9*, 51. https://doi.org/10.3390/chemosensors9030051

Academic Editor: Giovanni Neri

Received: 31 January 2021
Accepted: 1 March 2021
Published: 5 March 2021

1. Introduction

Low-dimensional metal oxide nanostructures have attracted considerable scientific interest due to their size and shape-dependent properties that can be tailored in a wide range. The inherently high surface-to-volume ratio makes them ideal candidates for various sensing applications, including gas sensors, humidity sensors, photodectors and biosensors [1]. Metal oxide semiconductors have a long history of scientific and industrial developments in the field of chemical sensing, ranging from initial discoveries in the 1950s and 1960s to continuous research efforts up to now, which also led to the successful realization of commercial sensor products. Whereas early work focused on leak detection and safety applications, current developments most commonly pursue the development of sensor devices for indoor and outdoor air quality monitoring, aiming at selective gas classification and quantitative determination of environmental pollutant concentrations. In addition to air quality monitoring, metal oxide-based gas sensors are also highly promising candidates for biomedical diagnostics based on exhaled breath analysis. Potential exemplary applications include the diagnosis of diabetes (acetone sensing), halitosis (hydrogen sulfide sensing) and lung cancer [2].

In this review, research progress on gas sensor devices based on copper oxide will be summarized—in particular, those employing cupric oxide (CuO) and cuprous oxide (Cu_2O) nanostructures. Among the large number of different metal oxides, these materials belong to the group of semiconductors with p-type conductivity resulting from unintentional doping that arises from non-stoichiometry [3]. Copper oxides are abundant and non-toxic materials that can be fabricated by sustainable low-cost processes. Different synthetic procedures are available to achieve nanomaterials with high crystalline quality, including their size and shape control, hence allowing for the realization of nanoelectronic devices with tailored properties. Apart from (bio)chemical sensors (see also reference [4] for a previous review on gas sensing applications), copper oxide has been employed in various areas—for instance, photovoltaics, lithium ion batteries, (photo)catalysis, electrochromic devices, supercapacitors, nanofluids, field emission devices and antimicrobial applications [5,6]. Here, the most important considerations for gas sensing applications,

including the basic mechanisms for sensing and transduction will be outlined, ranging from the design of the employed nanomaterials, to the structures of the sensor devices and the overall sensor systems. While most of these considerations are more general and also applicable to other material systems, the discussion will emphasize literature reports on copper oxide nanomaterials. Results on devices for chemical sensing in dry and humid air at atmospheric pressure will be considered, focusing on several target molecules, including volatile organic compounds (VOCs), hydrogen sulfide (H_2S), carbon monoxide (CO), carbon dioxide (CO_2), hydrogen (H_2) and nitrogen oxide (NO_x) from parts-per-million (ppm) down to parts-per-billion (ppb) concentrations. Note that this review covers gas sensors in which copper oxide nanostructures are the main "base" material, and literature reports on nanocomposites, core-shell structures, extended heterostructures, etc., are not discussed here. For a detailed comparison between different metal oxide materials for gas sensors, the reader is referred to [7].

2. Nanomaterial, Device and Sensor System Design

The following schematic diagram (Figure 1) illustrates the most important aspects that influence the properties of chemical sensor devices. To achieve rationally designed gas sensors with optimized performance tailored to the specific application, these influencing factors need to be considered when designing the nanomaterials, the device structure and the overall sensor system.

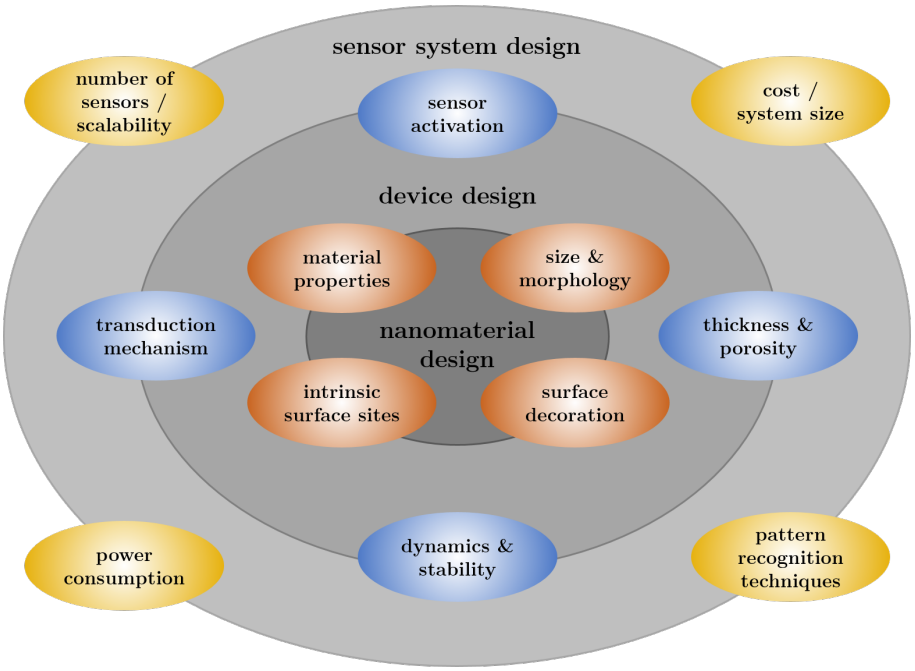

Figure 1. Schematic illustration of general factors influencing gas sensor properties, which need to be addressed by nanomaterial, device and sensor system design. This contribution aims at reviewing the respective aspects for copper oxide-based gas sensors reported in literature.

2.1. Influence of Copper Oxide Phase

Three different oxidation states and crystalline phases with distinct material properties can occur: cupric oxide CuO or Cu(II) oxide with monoclinic crystal structure, cuprous oxide Cu_2O or Cu(I) oxide with cubic crystal structure and paramelaconite Cu_4O_3, a mixture of Cu(II) and Cu(I) coordination, with tetragonal crystal structure. The reader is referred to the review articles in references [5,8] for a detailed discussion on the corresponding material properties. From a chemical sensing perspective the CuO and Cu_2O phases have been the most relevant, whereas the former is more stable at elevated temperatures and ambient pressure. Depending on environmental conditions, surface oxidation of Cu_2O

to CuO has to be taken into account, considering the thermodynamic stability of Cu_2O surfaces [9,10].

A systematic comparison between the gas sensitivity of CuO and Cu_2O is often difficult due to differences in synthetic procedures, which can lead to nanomaterials with different sizes or morphologies. The ethanol sensing properties of CuO thin films (nanocrystal dimensions ~30 nm) and Cu_2O thin films (nanocrystal dimensions ~85 nm) fabricated by reactive magnetron sputtering were compared [11]. The CuO thin films exhibited higher ethanol response, lower optimum operation temperature and shorter response/recovery times. In reference [12], ethanol sensing with thin film devices based on copper oxide nanocrystals was reported. Mixed copper oxide phases obtained by annealing treatments of Cu_2O layers showed superior ethanol sensing performance compared to single-phase materials, which was attributed to the formation of CuO–Cu_2O heterojunctions. Furthermore, CuO–Cu_2O composites with hollow single- and multi-shell morphologies presented enhanced ethanol response compared to their single-phase CuO counterparts [13].

2.2. Influence of Nanomaterial and Sensor Morphology

The choice of nanomaterial and sensor fabrication method is of utmost importance for achieving gas sensor devices with desired properties. The size and morphology of the employed nanostructures governs their surface-to-volume ratio, which is a crucial parameter to maximize the impact of surface reactions on the overall nanostructure's electrical conductivity. For instance, hierarchical nanostructures can be employed to maximize the surface-to-volume ratio and achieve sensor devices with superior sensitivity (see, e.g., reference [14] and multiple other examples summarized in Section 4). While the size and porosity of the initial nanomaterials play a decisive role, also the sensor preparation method will determine the thickness and porosity of the overall sensing layer. The nanoscale morphology will not only influence the gas sensitivity but also other parameters such as sensor dynamics and long-term stability due to the impact on gas diffusion processes and grain growth at elevated temperatures, respectively.

Single-crystalline nanowires have been extensively studied for gas sensing applications with the prospect of improved long-term stability compared to polycrystalline materials. CuO nanowire devices in various configurations have been realized, including single nanowires in four-point configuration [15,16], single suspended nanowires [17], nanowire networks obtained via thermal oxidation of adjacent microspheres [18] and nanowire networks realized by thermal oxidation of lithographically defined Cu microstructures [19,20]. In contrast to layers of nanostructured materials, devices based on individual single-crystalline nanowires do not contain grain boundaries or porosity, which has a profound impact on the sensor transduction mechanism. On the other hand, nanowire networks constitute an intermediate case where single-crystalline sensing elements are interconnected at the nanowire boundaries that are in mechanical contact.

A major advantage of using copper oxide nanomaterials for chemical sensing is the availability of synthesis methods with high degree of morphological control, in particular, size- and shape-controlled growth of Cu_2O micro- and nanostructures [21]. Homogeneous sensing materials with well-defined structures can be achieved either by directly employing as-synthesized Cu_2O or by using calcination processes to transform Cu_2O to CuO. Several examples for shape-dependent gas sensing properties have been reported: Octahedral Cu_2O particles with exposed [111] facets showed superior CO sensing properties compared to Cu_2O cubes with exposed [100] facets and truncated Cu_2O octrahedra [22]. Similarly, octahedral Cu_2O was favorable for ethanol, acetone, triethylamine and formaldehyde detection compared to Cu_2O cubes and the importance of 1-coordinated Cu atoms obtained via hydrogenation was highlighted [23]. On the other hand, Cu_2O cubes exhibited enhanced sensing performance for NO_2, acetone and benzene compared to octahedral Cu_2O [24]. In reference [25], the CO sensing performance of CuO nanotubes (exposed [111] planes; obtained by thermal oxidation of Cu nanowires) and CuO nanocubes (exposed [110] surface planes; obtained by thermal oxidation of Cu_2O nanocubes) were compared,

showing that higher sensitivity and lower sensor operation temperature could be achieved with CuO nanotubes.

2.3. Impurity Doping and Nanoparticle Decoration

The performances of metal oxide semiconductor-based gas sensors, in particular, their sensitivity, selectivity and stability, can be significantly influenced by the functionalization with additives such as noble metals, other metal oxides or carbon-based nanomaterials. The impact on the gas sensing properties is a result of a complex interplay between several physico-chemical processes, commonly subsumed under chemical and electronic sensitization. Thereby, it is crucial how the additive is introduced into the sensing layer, which can range from the incorporation of atoms in the nanostructure bulk or at its surface (impurity doping) to formation of additive clusters/nanoparticles at the nanostructure surface (nanoparticle decoration). As a result, the functionalization method needs to be carefully chosen and optimized to achieve the desired enhancement in sensor performance. For a detailed discussion on the resulting impact of additives on gas-solid interactions and sensor transduction, the reader is referred to a recent review article [26].

Here, selected examples of impurity doping and nanoparticle decoration of copper oxide nanomaterial-based sensors will be discussed. Substitutional doping of CuO hollow spheres with aliovalent Li(I) and Fe(III) was reported in [27], showing significant electronic modification of the sensing material. Fe(III) doping led to a reduction of the hole density and an increase of the ethanol gas response, whereas the opposite was observed for Li(I) doping. The authors of reference [28] found that Sn and Zn doping is suitable for improving the sensing response of CuO nanoparticle-based sensors to ethanol and acetone, respectively. The different effects of Sn and Zn doping were attributed to a change of active adsorption sites (prevalent for Sn doping) and to the formation of CuO-ZnO p-n heterojunctions (prevalent for Zn doping). In references [29,30], the influence of decorating CuO nanowire-based devices with TiO_2, NiO and Co_3O_4 nanoparticles was studied. The decoration with n-type TiO_2 and p-type Co_3O_4 resulted in an increase of sensor response for oxidizing gases and a decrease of sensor response for reducing gases, whereas the opposite effect was observed for decoration with p-type NiO. The impact of functionalization was explained by a modulation of the hole accumulation layer at the CuO surface by semiconductor-semiconductor heterojunctions. Moreover, the CO and NO_2 sensing performance of CuO nanowire-based devices could be significantly enhanced by Au nanoparticle decoration and the nanoparticle size was found to play a decisive role (optimum around 60 nm) [31]. In addition to improving sensitivity and gas selectivity, impurity doping and nanoparticle decoration are used to reduce the sensor's working temperature and thus its power consumption. For instance, Pd nanoparticle decoration reduced the optimum temperature for H_2S sensing of CuO nanowire-based sensors from 300 °C to 100 °C, which also enabled the device operation in self-heated mode [32]. Depending on the nanoparticle material used for CuO decoration, the possibility of nanoparticle oxidation at elevated temperatures in oxygen-containing atmosphere needs to be considered, which was studied for CuO nanowires decorated with Ru [33], Pd [34,35] and Pt [36] nanoparticles. It was shown that the interactions between the nanoparticles and the CuO support played an important role in determining the nanoparticle crystalline structure upon oxidation, the charge transfer processes occurring at the hetero-interfaces and the catalytic activity.

2.4. Advances in Scalable Device Integration: From Microhotplates to Flexible Substrates

The realization of smart sensor systems capable of gas and odor classification for indoor air quality monitoring requires the implementation of a large number of individual gas sensor elements to enable the use of pattern recognition techniques. Scalable manufacturing processes for the low-cost fabrication of miniaturized sensor devices are needed to achieve economic solutions with small system sizes. In this context, not only the active sensing structures but also additional elements for sensor activation, typically heating elements,

need to be considered. Over the last decades, so-called microhotplate devices have been developed for this purpose [37]. These micromachined structures show some similarities to MEMS and most commonly consist of a suspended membrane (size in the order of 100 µm) with an embedded resistive heater. The latter allows for local heating of the microhotplate membrane up to several hundred degrees at a power consumption of only tens of milliwatt. This technology opens up opportunities of dynamic heating protocols and large sensor arrays with devices operated individually at different operation temperatures.

Gas sensor devices based on copper oxide nanomaterials have been successfully implemented on microhotplate structures. Nanogranular CuO thin films directly deposited on microhotplate devices and structured by a photolithographic lift-off process showed a sensor response for acetaldehyde down to 2 ppm, which was significantly increased by a factor of 7 using dynamic heating protocols [38]. Alternatively, CuO nanoparticles can be deposited on microhotplates by inkjet printing, which resulted in devices for H_2 and H_2S sensing [39]. CuO nanowires can be grown by thermal oxidation of Cu microstructures via heating microhotplate devices in oxygen-containing atmosphere, which allows for well-controlled local nanowire synthesis and does not require to anneal the entire sample in a furnace or macroscopic hotplate setup. This approach enabled the direct integration of CuO nanowires as active sensing elements in situ inside a gas measurement setup, leading to highly sensitive devices for CO detection down to 1 ppm and to new insights on sensor deactivation processes [40]. Furthermore, local CuO nanowire growth was demonstrated on CMOS hotplates fabricated in an industrial process [41] and was suitable for achieving CO sensing down to a concentration of 10 ppm at a power consumption of only 18.2 mW [42]. Another option for integrating copper oxide nanomaterials with CMOS technology was demonstrated in reference [43], where CuO nanowires were realized by the thermal oxidation of Cu through-silicon via (TSV) and employed for VOC sensing. As copper is widely available in microelectronic fabrication environments and thermal oxidation to Cu_2O and CuO (and CuO nanowire growth) can be performed at moderate temperatures, the use of copper oxide nanomaterials is advantageous due to the potential for scalable fabrication of sensor devices using industrial processes.

In recent years, interest in portable low-cost gas sensors has significantly increased due to emerging applications in wearables, e-textiles and smart packaging, but flexible polymeric, paper or textile substrates introduce new technological challenges for sensor device fabrication and operation [44]. Most importantly, the sensing materials have to allow for low working temperatures and be able to maintain their performance/functionality under repeated mechanical bending/stretching. Several types of copper oxide nanomaterials suitable for synthesis, deposition and sensor operation at low temperatures have been developed (summarized in detail in the following section), which makes them promising candidates for wearable device technologies. High-performance gas sensors for acetone detection down to 50 ppb at 50% relative humidity were demonstrated by magnetron sputtering deposition of CuO thin films on flexible Kapton substrates [45].

3. Mechanisms for Sensing and Transduction

3.1. Surface Reactions and Transduction Mechanisms

The vast majority of literature reports on copper oxide-based gas sensors relies on conductometric transduction principles, which means that the electrical resistance of the active sensing structures changes upon gas exposure. Considering the chemisorption model for a p-type semiconductor in oxygen-containing atmosphere (see, e.g., recent reviews in references [46,47]), surface adsorption of oxygen leads to the trapping of electrons and the formation of a hole accumulation layer. During gas sensor operation, the hole accumulation layer (and consequently the potential barrier and the electrical conductivity at the surface) is influenced by gaseous analytes either via interactions with chemisorbed oxygen or via adsorption processes linked with charge transfer. Detailed theoretical modeling for the case of detecting reducing gases with p-type semiconductor gas sensors has clarified the influence of temperature, doping concentration, energetic position of surface acceptor

level, reducing gas activation energy and pressure [48]. Similar theoretical modeling was performed for the detection of oxidizing gases with p-type semiconductors and was compared with experimental results [49]. To understand the transduction of these surface reactions into electrical signals, the nanoscale morphology of the sensing structures has to be considered. The chemisorption model is well-established for nanocrystalline thin films, where the sensor conductance is exponentially dependent on the surface potential barrier [46]. It can be assumed that this framework is applicable for a wide range of loosely interconnected films of different copper oxide nanomaterials summarized in the following section. However, modifications will be required for sensor devices based on compact thin films [50] or single-crystalline nanowires [51].

Although the chemisorption model can successfully explain many experimental results observed for conductometric gas sensors, further details related to surface reactions and the sensing mechanism often remain elusive. In most cases, important information on the sensing material properties is missing, e.g., carrier concentration, surface defect densities, type of exposed surface facets, surface termination etc., especially under sensor operation conditions. To date, several reports on ab initio calculations for idealized CuO surfaces based on density functional theory are available, studying the interactions with H_2O, NO_2 [52], ethanol, 2-propanol, H_2 [53], H_2S [54] O_2, formaldehyde [55] and H_2 for Zn-doped CuO and Cu_2O surfaces [56]. However, future experimental studies employing prototypical model systems with well-defined properties will be required to bridge the gap towards an atomistic understanding of gas sensing processes.

It should be noted that copper oxide-based gas sensors using alternative transduction concepts have also been reported. The direct measurement of the metal oxide work function by means of a Kelvin probe [57] was employed for CO_2 detection with CuO nanoparticles [58–60]. Moreover, surface ionization readout was shown to be suitable for detecting dimethylamine, ethanol and ammonia using CuO nanowire electrodes [61].

3.2. Humidity Interference Effects

The influence of humidity on the gas sensing properties of metal oxide-based devices has been extensively investigated, particularly for tin oxide SnO_2, but is still not comprehensively understood to date. Recent studies employing infrared spectroscopy under operando conditions have highlighted the complexity of the interactions between water vapor and SnO_2 surfaces, discussing the possibility of multiple co-existing reaction pathways, dependencies on crystal facets and surface defects and temperature effects [62,63]. Unfortunately, considerably less information is available about the fundamental mechanisms governing humidity interference effects in copper oxide-based sensors. The gas sensing response of CuO-based devices was compared in dry and humid atmosphere in several literature reports on CO and H_2S sensing: Thick film devices consisting of CuO nanoparticles showed a significantly reduced CO response in humid atmopshere at a working temperature of 150 °C, which was explained by a competition between CO and H_2O molecules for chemisorbed oxygen reaction partners [64]. In contrast, a very low influence of humidity on the CO response of CuO nanowire-based devices operated at 325 °C was found [65]. Similarly, CO sensor devices relying on CuO nanotubes that were operated at 175 °C exhibited no marked humidity interference effects [25]. For the case of H_2S sensing, the sensing properties of CuO nanosheet-based devices were studied in dry and humid atmosphere at temperatures from 250–325 °C [66,67], showing high robustness of the sensor responses to humidity with more pronounced humidity interference at low temperatures and high relative humidity levels. On the other hand, decreased H_2S response in the presence of humidity was reported for sensors based on CuO nanoparticles (room temperature operation) [68] and CuO nanosheets (working temperature 240 °C) [69]. In contrast, enhanced H_2S response was observed for CuO nanowire devices operated at 325 °C in humid air compared to dry atmosphere, whereas the response was almost constant for different relative humidity levels [70]. These at first sight contradictory examples illustrate that further advances in understanding humidity interference effects in copper

oxide-based devices will be required to deliberately control or eliminate the influence of humidity on the sensing properties.

4. Highly Sensitive Detection of Gaseous Molecules

4.1. Volatile Organic Compounds (VOCs)

Volatile organic compounds (VOCs) are omnipresent in our daily lives, as they are produced from countless anthropogenic sources. Several VOCs have been identified as toxic and carcinogenic with multiple potential adverse health effects even at sub-ppb-level exposure. Apart from industrial process control, VOC sensors are particularly important for indoor air quality monitoring, which requires inexpensive real-time sensor solutions with high sensitivity and selectivity. The reader is referred to reference [71] for a detailed description of various VOCs and for a review on metal oxide-based sensors for their detection. Copper oxide nanomaterials have been extensively studied for realizing VOC sensor devices, which is summarized in Table 1. Most commonly, VOCs act as reducing gases that react with chemisorbed oxygen and consequently influence the space charge region at the metal oxide surface.

Table 1. A summary of sensing volatile organic compounds (VOCs) with copper oxide-based devices. If the detection of several VOCs was reported, the target VOC is marked with †.

Nanomaterial Morphology	Synthesis Method	Operation Temp. [° C]	Target VOC	VOC Gas Conc. [ppm]	Humid Atm.	Lit. Ref.
CuO nanosheets	thermal decomposition	100–440	formaldehyde †	0.01–1000	✓	[55]
CuO nanowires (Ru decor.)	thermal oxidation	200–300	acetone	0.025–0.2	×	[33]
CuO thin films	magnetron sputtering	50–350	acetone	0.05–1.25	✓	[45]
CuO nanocubes	oxidation of Cu_2O nanocubes	250–350	formaldehyde †	0.05–3	×	[72]
CuO nanoflowers	sol-gel method	160–320	formaldehyde †	0.05–1	✓	[73]
CuO nanoparticles	sol-gel method	180–290	acetone †	0.1–10	✓	[74]
porous CuO (Pt doped)	template-assisted	200–275	formaldehyde †	0.1–1.5	✓	[75]
CuO/Cu_2O nanopatterns (Ag decor.)	thermal oxidation	200–350	acetone †	0.125–1000	×	[76]
CuO thin films (Cr doped)	magnetron sputtering	150–500	acetone †	0.32–3.2	✓	[77]
facet-controlled Cu_2O	wet chemical	100–250	benzene/acetone	1–10	×	[24]
CuO nanowires	thermal oxidation	300	benzene/toluene	1–10	×	[20]
CuO nanowires (NiO decor.)	thermal oxidation	300	benzene/toluene	1–10	×	[30]
CuO nanoparticles (Zn doped)	wet chemical	100–350	acetone †	1–20	×	[28]
CuO nanowires (Au decor.)	thermal oxidation	350	benzene/toluene	1–50	×	[31]
CuO particles	hydrothermal	230	decane †	1–100	×	[78]
hollow CuO nanofibers	template-assisted	140–260	n-propanol †	1–100	×	[79]
CuO nanosheets	hydrothermal	100–300	ethanol	1–100	×	[80]
CuO polyhedrons (PtO_2 decor.)	template-assisted	100–220	butanol †	1–500	×	[81]
CuO nanowires	template-assisted	130–260	n-propanol †	1–500	×	[82]
CuO thin films	magnetron sputtering	dynamic	acetaldehyde	2–5	✓	[38]
CuO nanowalls	wet chemical oxidation	200–360	acetone †	2–500	×	[83]
wormlike CuO structures	calcination of precursor	140–340	ethanol †	2–800	✓	[84]
CuO nanowires	thermal oxidation	150–400	butanol †	3–30	✓	[85]
CuO nanoplatelets	hydrothermal	25–150	xylene †	5–100	×	[86]
CuO nanowires	thermal oxidation	150–400	ethanol	5–100	✓	[87]
Cu_2O octahedrons	wet chemical	100–260	ethanol †	5–500	×	[23]
CuO nanoribbons (Au and Pt decor.)	hydrothermal	200	formaldehyde †	5–500	×	[88]
CuO nanoparticles	calcination of precursor	150–300	ethanol	5–1000	×	[89]
Cu_2O octahedral nanoparticles	wet chemical	170–290	benzene †	5–1000	×	[90]
porous CuO particles	calcination of precursor	230	triethylamine †	5–1000	×	[91]
hollow Cu_2O polyhedrons	wet chemical	130–310	ethanol	5–4000	×	[92]
porous Cu_2O spheres	wet chemical	160–300	ethanol †	5–5000	×	[93]
Cu_2O nanocrystals	hydrothermal	dynamic	ethanol	10–100	×	[94]
CuO/Cu_2O nanocrystalline films	chemical synthesis/annealing	25–350	ethanol	10–100	×	[12]

Table 1. *Cont.*

Nanomaterial Morphology	Synthesis Method	Operation Temp. [° C]	Target VOC	VOC Gas Conc. [ppm]	Humid Atm.	Lit. Ref.
CuO nanoplatelets	hydrothermal	25–100	2-propanol	10–100	×	[95]
single CuO nanowire	thermal oxidation	room temp.	ethanol	10–100	✓	[87]
CuO nanosheets	hydrothermal	270–370	ethanol †	10–200	×	[96]
CuO nanoflowers (In doped)	hydrothermal	95–180	ethanol †	10–300	✓	[97]
dodecahedral Cu_2O nanocages	wet chemical	150–300	ethanol †	10–300	×	[98]
CuO and Cu_2O nanospheres	wet chemical	210	ethanol	10–800	×	[99]
CuO nanoflowers	microwave-assisted	150–400	ethyl-acetate †	10–1000	✓	[100]
CuO nanosheets	calcination of precursor	170–370	ethanol †	10–2000	×	[101]
CuO and Cu_2O thin films	magnetron sputtering	120–320	ethanol	12.5–500	×	[11]
CuO nanoparticles	thermal oxidation	200	ethanol †	20–500	×	[102]
CuO nanowires	thermal oxidation	150–300	ethanol	25–1000	×	[103]
CuO nanowires	thermal oxidation	300	ethanol †	25–1000	×	[43]
porous Cu_2O cubes	hydrothermal	250	ethanol	50–250	×	[104]
CuO thin film	wet chemical	200–300	2-propanol †	50–300	✓	[105]
porous CuO/Cu_2O cubes	calcination of precursor	100–220	acetone †	50–500	×	[106]
CuO hollow spheres	calcination of precursor	200–400	ethanol	50–1000	×	[107]
CuO/Cu_2O hollow spheres	template-assisted	80–160	ethanol	50–1000	×	[13]
CuO hollow spheres (Fe doped)	calcination of precursor	200–400	ethanol	50–1000	×	[27]
mesoporous CuO films	calcination of precursor	300–400	ethanol	100–1000	×	[108]

4.2. Hydrogen Sulfide (H_2S)

The occurrence of hydrogen sulfide (H_2S) can be a result of bacterial decomposition of organic matter in anaerobic environments including natural sources or originate from a large variety of industrial processes. This corrosive and toxic gas is characterized by a 'rotten egg' smell at an odor threshold in the low ppb range while at higher concentrations it can paralyze the olfactory nerves. Due to the high toxicity, H_2S exposure can lead to headache, nausea, unconsciousness and suffocation, whereas increased odds ratio for central nervous and respiratory symptoms can be a result of long-term ppb-level exposure. With suggested exposure limits in the low ppm range, stringent sensitivity requirements are placed on H_2S sensors that have triggered considerable efforts for developing suitable metal oxide-based devices [109]. Copper oxide nanomaterials have shown excellent sensitivity (and often selectivity) to H_2S with low detection limits of 1 ppb and below [68,110]. Further literature reports on H_2S sensors employing copper oxide nanomaterials are summarized in Table 2. At elevated temperatures the detection mechanism of H_2S is attributed to reactions with chemisorbed oxygen to form SO_2 and H_2O, whereas at low temperatures the formation of CuS is dominant which can lead to irreversible changes of the nanomaterial structure. The latter was further substantiated by near-edge X-ray absorption fine structure spectroscopy in combination with X-ray microscopy [111]. CuS formation can result in low-resistance percolation pathways leading to a dramatic increase in sensor conductivity, which was demonstrated for CuO nanoparticle-based sensing layers [112] and CuO nanowire-based devices [19]. The phase transition to CuS can be utilized as alternative transduction principle for operating copper oxide-based sensors as dosimeter-type devices that assess the product of H_2S concentration and exposure time [113–115]. Detailed analysis of the sensor response has led to further insights in percolation and diffusion processes [113,114] and it will be an interesting direction for future studies to assess if similar phase transition-based transduction concepts can be employed for other target gases or nanomaterial systems.

Table 2. A summary of sensing hydrogen sulfide (H_2S) with copper oxide-based devices.

Nanomaterial Morphology	Synthesis Method	Operation Temp. [° C]	H_2S Gas Conc. [ppm]	Humid Atm.	Lit. Ref.
CuO nanoparticles	hydrothermal	20–120	0.0001–1	✓	[68]
CuO nanowires	thermal oxidation	325	0.001–0.5	×	[110]
single CuO nanowire	thermal oxidation	325	0.01–0.5	✓	[70]
CuO nanowires	thermal oxidation	325	0.01–0.5	✓	[70]
porous CuO nanobelts	calcination of precursor	125–225	0.01–5	×	[116]
CuO nanosheets	hydrothermal	room temp.	0.01–60	×	[117]
CuO nanowires	template-assisted	25–420	0.01–1	×	[118]
CuO nanosheets	hydrothermal	90–300	0.03–1.2	✓	[69]
porous CuO spheres	hydrothermal	90–300	0.03–1.2	×	[119]
CuO/Cu_2O nanoparticles	hydrothermal	80–180	0.05–1	✓	[120]
CuO nanospindles	hydrothermal/annealing	dynamic	0.1–1	×	[121]
CuO nanowires (Fe_2O_3 decor.)	thermal oxidation	50–250	0.1–5	×	[122]
CuO thin films	thermal oxidation	room temp.	0.1–10	×	[123]
CuO nanobelts	sonochemical	100–220	0.1–10	✓	[124]
CuO nanoflowers (Pt doping)	hydrothermal	dynamic	0.1–10	×	[125]
CuO nanoflowers	hydrothermal	room temp.	0.1–20	×	[126]
CuO nanoflowers (Pd doped)	hydrothermal	70–340	0.1–50	×	[127]
CuO colloidal particles	oxidation of Cu_2O particles	dynamic	0.1–100	✓	[128]
CuO nanosheets	hydrothermal	250–325	0.2–5	✓	[67]
CuO nanosheets	hydrothermal	150–300	0.2–10	✓	[66]
single CuO nanowire	thermal oxidation	200–300	0.5–10	×	[15]
CuO nanoparticles	inkjet printing	dynamic	0.5–10	✓	[115]
CuO nanoplates	hydrothermal	250–350	1–10	×	[129]
CuO nanofibers (RGO [a] loaded)	calcination of precursor	150–400	1–10	×	[130]
CuO hollow spheres	calcination of precursor	200–400	1–20	×	[107]
CuO nanofibers	calcination of precursor	room temp.	1–100	✓	[131]
CuO nanoparticles	inkjet printing	350–450	3–15	×	[39]
porous Cu_2O hexapods	hydrothermal	80–260	5–5000	×	[132]
CuO nanorods (Pd decor.)	thermal oxidation	300	20–100	×	[133]

[a] reduced graphene oxide.

4.3. Carbon Monoxide (CO)

Carbon monoxide (CO) is a major environmental pollutant resulting from incomplete fuel combustion, occurring for example in industrial processes, automotive emissions and fuel-based household appliances. It is an odorless, colorless and toxic gas with a strong affinity to bind with hemoglobin in human blood, reducing the ability of oxygen transport within the body. Exposure to a concentration of 10 ppm CO is considered acceptable within a time of 8 h, whereas higher concentrations can lead to symptoms such as headache, confusion, unconsciousness and death with a significant number of fatalities from CO poisoning constantly occurring worldwide. Consequently, the development of high-performance CO sensors has been an active field of research for decades with metal oxide semiconductors being among the most widely studied materials for the realization of chemoresistive sensor devices [134]. A summary of literature reports on CO sensor devices based on copper oxide nanomaterials is shown in Table 3. The sensing mechanism in air is typically explained by a reaction with chemisorbed oxygen to form CO_2, leading to a modulation of the surface space charge region.

Table 3. A summary of sensing carbon monoxide (CO) with copper oxide-based devices.

Nanomaterial Morphology	Synthesis Method	Operation Temp. [° C]	CO Gas Conc. [ppm]	Humid Atm.	Lit. Ref.
CuO nanowires	thermal oxidation	300	1–10	×	[20]
CuO nanowires (NiO decor.)	thermal oxidation	300	1–10	×	[30]
CuO nanowires	thermal oxidation	325	1–30	×	[40]
CuO nanowires (Au decor.)	thermal oxidation	200–400	1–50	×	[31]
octahedral Cu_2O particles	wet chemical	50–120	1–800	×	[22]
CuO nanofibers	calcination of precursor	300	3–150	×	[135]
CuO powder	plasma spraying	100–350	5–500	×	[136]
CuO nanowires	thermal oxidation	25–350	5–1200	×	[137]
CuO nanoplatelets	hydrothermal	room temp.	10–100	✓	[138]
CuO nanoparticles	wet chemical	150	10–100	✓	[64]
CuO nanowires	thermal oxidation	300	10–100	×	[19]
CuO nanowires	thermal oxidation	300–370	10–100	×	[139]
single CuO nanowire	thermal oxidation	350	10–100	×	[17]
Cu_2O/Au/CuO nanostructures	wet chemical	200	10–500	×	[140]
CuO nanowires (Pt decor.)	thermal oxidation	200–250	15–45	×	[35]
CuO nanowires	thermal oxidation	300–350	25–150	✓	[65]
CuO nanoleaves (Al doped)	wet chemical	70–230	35–12,500	✓	[141]
single CuO nanowire	thermal oxidation	350	50–150	✓	[142]
CuO nanocubes	oxidation of Cu_2O nanocubes	100–300	50–1000	×	[25]
CuO nanotubes	oxidation of Cu nanowires	100–300	50–1000	✓	[25]
single CuO nanowire (Pd decor.)	thermal oxidation	350	100–300	✓	[143]
CuO nanowires	thermal oxidation	30–400	100–1000	×	[144]
CuO nanoparticles	hydrothermal	150–400	200–1000	×	[145]

4.4. Carbon Dioxide (CO_2)

Despite active research efforts for several decades, the realization of miniaturized sensor solutions for detecting carbon dioxide (CO_2) based on solid-state materials has remained challenging. Current technologies often rely on optical sensing principles, which comes at the expense of elevated cost and power consumption combined with large sensor system size. Different types of solid-state electro-chemical sensors including resistive sensors based on metal oxide semiconductors have been developed as potential low-cost alternatives [146]. Copper oxide nanomaterials have shown highly promising prospects in this regard: In addition to perovskite-based nanocomposites (e.g., Ag-doped CuO/$BaTiO_3$ heterostructures: [146,147] and references therein) and CuO/$CuFe_2O_4$ nanocomposites [148], CuO nanoparticle-based sensors relying on work function readout were found to be capable of detecting CO_2 in humid atmosphere at low working temperatures down to room temperature in the application-relevant concentration range (400–4000 ppm) [58–60]. Moreover, resistive gas sensors based on CuO nanoparticles with ZnO_2 additives [149] and Au-decorated CuO thin films [150] have been reported, showing similar capabilities with high practical importance. Hence, future developments and improvements of copper oxide

nanomaterial-based sensors could result in miniaturized low-cost CO_2 sensor solutions that find widespread real-world applications with significant industrial relevance. Examples include next-generation greenhouse gas sensors for monitoring industrial CO_2 emissions and outdoor air quality [146], and indoor air quality control in smart homes/Internet of Things applications [151]. Furthermore, the development of portable low-cost CO_2 sensors would have significant impacts on the agriculture and food industry, as they could be integrated into intelligent packaging to enhance food quality and safety [152].

4.5. Hydrogen (H_2)

With the emergence of the hydrogen economy relying on this abundant element for sustainable fuels and energy storage, the detection of hydrogen (H_2) gas has reached an unprecedented level of importance. H_2 leakage detection is required in related applications due to the flammable and explosive nature of this gas in a wide concentration range. A large number of metal oxide semiconductors have been successfully employed for realizing chemoresistive sensor devices for detecting this reducing gas [153]. In Table 4, a summary of literature reports on H_2 sensor devices based on copper oxide nanomaterials is presented. Resistance changes during H_2 exposure are attributed to reactions with chemisorbed oxygen to form H_2O molecules, influencing the charge carrier density close to the surface. Alternative transduction concepts have been proposed, including metallic percolation pathways in CuO nanowire-based sensors [154] and changes in the thermal properties of microhotplate devices [39]. Monitoring changes in the thermal properties of micromachined sensing structures constitutes a powerful strategy for future gas selectivity improvements, which can also be applied for other sensing materials.

Table 4. A summary of sensing nitrogen oxide H_2 with copper oxide-based devices.

Nanomaterial Morphology	Synthesis Method	Operation Temp. [° C]	H_2 Gas Conc. [ppm]	Humid Atm.	Lit. Ref.
CuO nanowires	thermal oxidation	300	1–10	×	[20]
CuO nanowires (NiO decor.)	thermal oxidation	300	1–10	×	[30]
CuO/Cu_2O nanocrystals (Zn doped)	wet chemical/annealing	100–450	10–100	✓	[56]
urchin-like CuO particles	microwave-assisted	150–400	10–500	×	[14]
CuO nanoparticles	inkjet printing	400	40–3000	×	[39]
CuO hollow spheres	calcination of precursor	200–400	50–1000	×	[107]
CuO nanowires	thermal oxidation	275–400	100	×	[154]
mesoporous CuO films	calcination of precursor	200–400	100–1000	×	[108]

4.6. Nitrogen Dioxide (NO_2)

Nitrogen dioxide (NO_2) contributes significantly to environmental pollution, being linked with smog and acid rain and adverse human health effects. Typically suggested exposure limits lie in the low ppm range, but continuous exposure at even lower levels can lead to respiratory symptoms and lung damage, especially in patients with preconditions. Anthropogenic production of nitrogen oxides is primarily related to fuel combustion, particularly from automotive emissions and industrial sources. Considering the current global status of air quality and pollution, there is a high and continuously increasing demand for NO_2 sensor devices, which can be realized with various metal oxide semiconductors [155]. Copper oxide nanomaterials often show excellent sensitivity to NO_2, as very low concentrations down to 1 ppb could be detected even for room temperature sensor operation [52]. Further literature reports on copper oxide-based NO_2 sensors are summarized in Table 5. NO_2 is a strongly oxidizing gas with high electron affinity that affects the space charge region at the metal oxide surface via charge transfer upon adsorption, whereas alternative processes can occur at elevated temperatures [156].

Table 5. A summary of sensing nitrogen dioxide (NO_2) with copper oxide-based devices.

Nanomaterial Morphology	Synthesis Method	Operation Temp. [° C]	NO_2 Gas Conc. [ppm]	Humid Atm.	Lit. Ref.
Cu_2O/CuO nanoflowers	wet chemical	room temp.	0.001–50	✓	[52]
Cu_2O/CuO octahedrons	calcination of precursor	room temp.	0.01–1	✓	[157]
facet-controlled Cu_2O	wet chemical	50–250	0.1–5	×	[24]
CuO nanoparticles	inkjet printing	120–500	0.2–5	✓	[156]
CuO nanowires	thermal oxidation	325	0.5–1.5	×	[40]
Cu_2O nanopatterns (Pt decor.)	thermal oxidation	300	1–5	×	[158]
CuO nanowires	thermal oxidation	300	1–10	×	[20]
CuO nanowires (TiO_2 decor.)	thermal oxidation	300	1–10	×	[29]
CuO nanowires (Co_3O_4 decor.)	thermal oxidation	300	1–10	×	[30]
porous CuO nanocubes	calcination of precursor	250–350	1–10	×	[159]
CuO nanofibers	calcination of precursor	300	1–20	×	[135]
CuO nanowires (Au decor.)	thermal oxidation	200–400	1–50	×	[31]
CuO nanowires	thermal oxidation	200–400	1–100	×	[139]
CuO nanocubes	thermal oxidation	100–250	1–100	×	[160]
CuO thin films (La_2O_3 doped)	spray pyrolysis	room temp.	1.5	✓	[161]
Cu_2O octahedral nanoparticles	wet chemical	50	5–50	×	[90]
CuO nanoparticles	hydrothermal	50–150	5–50	×	[162]
CuO nanostructures (Cr doped)	wet chemical	250–400	5–100	×	[163]
CuO nanoplatelets	hydrothermal	25–100	10–100	✓	[95]

4.7. Other Target Molecules

Highly sensitive devices for ozone O_3 detection at concentrations of 50–300 ppb in dry air were shown using CuO thin films realized by reactive magnetron sputtering combined with annealing [49]. Similarly, CuO nanowire-based devices synthesized by thermal oxidation were able to detect 50–300 ppb O_3 at 50% relative humidity [164].

Sulfur dioxide SO_2 sensing at a concentration range of 1–10 ppm in dry air was reported using CuO nanowires [20], CuO nanowires decorated with TiO_2 [29], CuO nanowires decorated with Co_3O_4 and NiO [30] and CuO nanoplates [129].

Ammonia NH_3 detection with single CuO nanowire devices was shown at concentrations of 1–10 ppm [15] and 1% [165] in dry air. Enhanced sensor performance was demonstrated by doping and nanoparticle decoration—in particular, Cr doping of CuO nanoboats (100–600 ppm concentration range) [166], CuO nanowires decorated with SnO_2 (1% concentration) [167] and CuO nanofibers decorated with In_2O_3 (0.3–100 ppm concentration range) [131].

Methane CH_4 was detected with Cu_2O thin films at concentrations of 0.3–2.5% [168].

5. Conclusions

To summarize, copper oxide nanomaterials have been widely applied to achieve high-performance gas sensor devices for the detection of the most common hazardous gases and environmental pollutants. In many cases excellent sensitivity with detection limits down to ppb-level concentrations or below could be accomplished. As for other metal oxide-based sensors, the gas selectivity of copper oxide-based devices has, however, remained limited despite some promising reports on doping and nanoparticle decoration, which often prevents the practical use in real-world applications. In this regard, a way forward would be to aim for further advances in realizing smart sensor systems, employing a large number of sensor devices and relying on pattern recognition techniques, machine learning, neural networks and artificial intelligence for gas and odor classification [169,170]. For example, unsupervised principal component analysis has been successfully applied for analyzing resistance transients of CuO thin film devices for distinguishing between four different VOCs (ethanol, methanol, acetone and 2-propanol) [105]. Another option would be the use of gas-selective pre-filters, for instance, to minimize the influence of H_2S or SO_2 exposure.

In addition to further technological developments, several fundamental scientific questions need to be addressed, particularly those related to the underlying mechanisms of humidity and target gas interactions with copper oxide surfaces, and the role of additives

for sensor functionalization. For this purpose, experimental techniques that allow for sensor material characterization under environmental conditions resembling sensor operation will play a crucial role, particularly infrared spectroscopy performed in operando [26,62,63]. In situ experiments of functional chemoresistive sensor devices inside environmental transmission electron microscopes [171,172] could provide new insights in changes of morphology and/or chemical composition of the employed nanostructures induced by exposure to reactive gas species at elevated temperatures. Moreover, in situ X-ray absorption spectroscopy [173] and near-ambient pressure X-ray photoelectron spectroscopy [174] have been successfully employed for correlating chemoresistive sensor responses with changes in the oxidation state of copper oxide nanomaterials. It can be expected that future technology and fundamental science advances will cross-fertilize to enable the rational design of copper oxide-based nanomaterials for chemoresistive sensors with improved performance.

Funding: The author acknowledges financial support from the Swedish Research Council for Sustainable Development (Formas, grant number 2019-01353).

Institutional Review Board Statement: Not applicable.

Informed Consent Statement: Not applicable.

Data Availability Statement: Not applicable.

Conflicts of Interest: The author declares no conflict of interest.

References

1. Nunes, D.; Pimentel, A.; Gonçalves, A.; Pereira, S.; Branquinho, R.; Barquinha, P.; Fortunato, E.; Martins, R. Metal oxide nanostructures for sensor applications. *Semicond. Sci. Technol.* **2019**, *34*, 043001. [CrossRef]
2. Moseley, P.T. Progress in the development of semiconducting metal oxide gas sensors: A review. *Meas. Sci. Technol.* **2017**, *28*, 082001. [CrossRef]
3. Kim, H.J.; Lee, J.H. Highly sensitive and selective gas sensors using p-type oxide semiconductors: Overview. *Sens. Actuators B Chem.* **2014**, *192*, 607–627. [CrossRef]
4. Rydosz, A. The Use of Copper Oxide Thin Films in Gas-Sensing Applications. *Coatings* **2018**, *8*, 425. [CrossRef]
5. Zoolfakar, A.S.; Rani, R.A.; Morfa, A.J.; O'Mullane, A.P.; Kalantar-zadeh, K. Nanostructured copper oxide semiconductors: A perspective on materials, synthesis methods and applications. *J. Mater. Chem. C* **2014**, *2*, 5247–5270. [CrossRef]
6. Zhang, Q.; Zhang, K.; Xu, D.; Yang, G.; Huang, H.; Nie, F.; Liu, C.; Yang, S. CuO nanostructures: Synthesis, characterization, growth mechanisms, fundamental properties, and applications. *Prog. Mater. Sci.* **2014**, *60*, 208–337. [CrossRef]
7. Eranna, G.; Joshi, B.C.; Runthala, D.P.; Gupta, R.P. Oxide Materials for Development of Integrated Gas Sensors—A Comprehensive Review. *Crit. Rev. Solid State Mater. Sci.* **2004**, *29*, 111–188. [CrossRef]
8. Meyer, B.K.; Polity, A.; Reppin, D.; Becker, M.; Hering, P.; Klar, P.J.; Sander, T.; Reindl, C.; Benz, J.; Eickhoff, M.; et al. Binary copper oxide semiconductors: From materials towards devices. *Phys. Status Solidi B* **2012**, *249*, 1487–1509. [CrossRef]
9. Soon, A.; Todorova, M.; Delley, B.; Stampfl, C. Thermodynamic stability and structure of copper oxide surfaces: A first-principles investigation. *Phys. Rev. B* **2007**, *75*, 125420. [CrossRef]
10. Gattinoni, C.; Michaelides, A. Atomistic details of oxide surfaces and surface oxidation: The example of copper and its oxides. *Surf. Sci. Rep.* **2015**, *70*, 424–447. [CrossRef]
11. Zoolfakar, A.S.; Ahmad, M.Z.; Rani, R.A.; Ou, J.Z.; Balendhran, S.; Zhuiykov, S.; Latham, K.; Wlodarski, W.; Kalantar-zadeh, K. Nanostructured copper oxides as ethanol vapour sensors. *Sens. Actuators B Chem.* **2013**, *185*, 620–627. [CrossRef]
12. Lupan, O.; Cretu, V.; Postica, V.; Ababii, N.; Polonskyi, O.; Kaidas, V.; Schütt, F.; Mishra, Y.K.; Monaico, E.; Tiginyanu, I.; et al. Enhanced ethanol vapour sensing performances of copper oxide nanocrystals with mixed phases. *Sens. Actuators B Chem.* **2016**, *224*, 434–448. [CrossRef]
13. Xu, J.; Yao, X.; Wei, W.; Wang, Z.; Yu, R. Multi-shelled copper oxide hollow spheres and their gas sensing properties. *Mater. Res. Bull.* **2017**, *87*, 214–218. [CrossRef]
14. Volanti, D.P.; Felix, A.A.; Orlandi, M.O.; Whitfield, G.; Yang, D.J.; Longo, E.; Tuller, H.L.; Varela, J.A. The Role of Hierarchical Morphologies in the Superior Gas Sensing Performance of CuO-Based Chemiresistors. *Adv. Funct. Mater.* **2013**, *23*, 1759–1766. [CrossRef]
15. Shao, F.; Hernández-Ramírez, F.; Prades, J.; Fàbrega, C.; Andreu, T.; Morante, J. Copper (II) oxide nanowires for p-type conductometric NH_3 sensing. *Appl. Surf. Sci.* **2014**, *311*, 177–181. [CrossRef]
16. Steinhauer, S.; Köck, A.; Gspan, C.; Grogger, W.; Vandamme, L.K.J.; Pogany, D. Low-frequency noise characterization of single CuO nanowire gas sensor devices. *Appl. Phys. Lett.* **2015**, *107*, 123112. [CrossRef]
17. Steinhauer, S.; Brunet, E.; Maier, T.; Mutinati, G.; Köck, A.; Freudenberg, O. Single Suspended CuO Nanowire for Conductometric Gas Sensing. *Procedia Eng.* **2012**, *47*, 17–20. [CrossRef]

18. Siebert, L.; Lupan, O.; Mirabelli, M.; Ababii, N.; Terasa, M.I.; Kaps, S.; Cretu, V.; Vahl, A.; Faupel, F.; Adelung, R. 3D-Printed Chemiresistive Sensor Array on Nanowire CuO/Cu2O/Cu Heterojunction Nets. *ACS Appl. Mater. Interfaces* **2019**, *11*, 25508–25515. [CrossRef]
19. Steinhauer, S.; Brunet, E.; Maier, T.; Mutinati, G.; Köck, A.; Freudenberg, O.; Gspan, C.; Grogger, W.; Neuhold, A.; Resel, R. Gas sensing properties of novel CuO nanowire devices. *Sens. Actuators B Chem.* **2013**, *187*, 50–57. [CrossRef]
20. Kim, J.H.; Katoch, A.; Choi, S.W.; Kim, S.S. Growth and sensing properties of networked p-CuO nanowires. *Sens. Actuators B Chem.* **2015**, *212*, 190–195. [CrossRef]
21. Sun, S.; Zhang, X.; Yang, Q.; Liang, S.; Zhang, X.; Yang, Z. Cuprous oxide (Cu_2O) crystals with tailored architectures: A comprehensive review on synthesis, fundamental properties, functional modifications and applications. *Prog. Mater. Sci.* **2018**, *96*, 111–173. [CrossRef]
22. Wang, L.; Zhang, R.; Zhou, T.; Lou, Z.; Deng, J.; Zhang, T. P-type octahedral Cu_2O particles with exposed 111 facets and superior CO sensing properties. *Sens. Actuators B Chem.* **2017**, *239*, 211–217. [CrossRef]
23. Chen, M.; Wang, Y.; Zhang, Y.; Yuan, Y.; Liu, J.; Liu, B.; Du, Q.; Ren, Y.; Yang, H. Hydrogenated Cu_2O octahededrons with exposed 111 facets: Enhancing sensing performance and sensing mechanism of 1-coordinated Cu atom as a reactive center. *Sens. Actuators B Chem.* **2020**, *310*, 127827. [CrossRef]
24. Xie, Z.; Han, N.; Li, W.; Deng, Y.; Gong, S.; Wang, Y.; Wu, X.; Li, Y.; Chen, Y. Facet-dependent gas sensing properties of Cu_2O crystals. *Phys. Status Solidi A* **2017**, *214*, 1600904. [CrossRef]
25. Hou, L.; Zhang, C.; Li, L.; Du, C.; Li, X.; Kang, X.F.; Chen, W. CO gas sensors based on p-type CuO nanotubes and CuO nanocubes: Morphology and surface structure effects on the sensing performance. *Talanta* **2018**, *188*, 41–49. [CrossRef]
26. Degler, D.; Weimar, U.; Barsan, N. Current Understanding of the Fundamental Mechanisms of Doped and Loaded Semiconducting Metal-Oxide-Based Gas Sensing Materials. *ACS Sens.* **2019**, *4*, 2228–2249. [CrossRef]
27. Choi, Y.H.; Kim, D.H.; Hong, S.H. p-Type aliovalent Li(I) or Fe(III)-doped CuO hollow spheres self-organized by cationic complex ink printing: Structural and gas sensing characteristics. *Sens. Actuators B Chem.* **2017**, *243*, 262–270. [CrossRef]
28. Hemalatha, T.; Akilandeswari, S.; Krishnakumar, T.; Leonardi, S.G.; Neri, G.; Donato, N. Comparison of Electrical and Sensing Properties of Pure, Sn- and Zn-Doped CuO Gas Sensors. *IEEE Trans. Instrum. Meas.* **2019**, *68*, 903–912. [CrossRef]
29. Choi, S.W.; Katoch, A.; Kim, J.H.; Kim, S.S. A novel approach to improving oxidizing-gas sensing ability of p-CuO nanowires using biased radial modulation of a hole-accumulation layer. *J. Mater. Chem. C* **2014**, *2*, 8911–8917. [CrossRef]
30. Choi, S.W.; Katoch, A.; Kim, J.H.; Kim, S.S. Remarkable Improvement of Gas-Sensing Abilities in p-type Oxide Nanowires by Local Modification of the Hole-Accumulation Layer. *ACS Appl. Mater. Interfaces* **2015**, *7*, 647–652. [CrossRef]
31. Lee, J.S.; Katoch, A.; Kim, J.H.; Kim, S.S. Effect of Au nanoparticle size on the gas-sensing performance of p-CuO nanowires. *Sens. Actuators B Chem.* **2016**, *222*, 307–314. [CrossRef]
32. Kim, J.Y.; Lee, J.H.; Kim, J.H.; Mirzaei, A.; Woo Kim, H.; Kim, S.S. Realization of H_2S sensing by Pd-functionalized networked CuO nanowires in self-heating mode. *Sens. Actuators B Chem.* **2019**, *299*, 126965. [CrossRef]
33. Porkovich, A.; Ziadi, Z.; Kumar, P.; Kioseoglou, J.; Jian, N.; Weng, L.; Steinhauer, S.; Vernieres, J.; Grammatikopoulos, P.; Sowwan, M. In Situ Observation of Metal to Metal Oxide Progression: A Study of Charge Transfer Phenomenon at Ru–CuO Interfaces. *ACS Nano* **2019**, *13*, 12425–12437. [CrossRef]
34. Steinhauer, S.; Zhao, J.; Singh, V.; Pavloudis, T.; Kioseoglou, J.; Nordlund, K.; Djurabekova, F.; Grammatikopoulos, P.; Sowwan, M. Thermal Oxidation of Size-Selected Pd Nanoparticles Supported on CuO Nanowires: The Role of the CuO–Pd Interface. *Chem. Mater.* **2017**, *29*, 6153–6160. [CrossRef]
35. Ziadi, Z.; Porkovich, A.J.; Kumar, P.; Datta, A.; Danielson, E.; Singh, V.; Sasaki, T.; Sowwan, M. Electronic Metal–Support Interactions at the Catalytic Interfaces of CuO Nanowires Decorated with Pt Nanoparticles for Methanol Oxidation and CO Sensing. *ACS Appl. Nano Mater.* **2020**, *3*, 8257–8267. [CrossRef]
36. Datta, A.; Deolka, S.; Kumar, P.; Ziadi, Z.; Sasaki, T.; Steinhauer, S.; Singh, V.; Jian, N.; Danielson, E.; Porkovich, A.J. In situ investigation of oxidation across a heterogeneous nanoparticle-support interface during metal support interactions. *Phys. Chem. Chem. Phys.* **2021**. [CrossRef] [PubMed]
37. Liu, H.; Zhang, L.; Li, K.H.H.; Tan, O.K. Microhotplates for Metal Oxide Semiconductor Gas Sensor Applications—Towards the CMOS-MEMS Monolithic Approach. *Micromachines* **2018**, *9*, 557. [CrossRef]
38. Presmanes, L.; Thimont, Y.; El Younsi, I.; Chapelle, A.; Blanc, F.; Talhi, C.; Bonningue, C.; Barnabé, A.; Menini, P.; Tailhades, P. Integration of P-CuO Thin Sputtered Layers onto Microsensor Platforms for Gas Sensing. *Sensors* **2017**, *17*, 1409. [CrossRef] [PubMed]
39. Bierer, B.; Kneer, J.; Wöllenstein, J.; Palzer, S. MEMS based metal oxide sensor for simultaneous measurement of gas induced changes of the heating power and the sensing resistance. *Microsyst. Technol.* **2016**, *22*, 1855–1863. [CrossRef]
40. Steinhauer, S.; Chapelle, A.; Menini, P.; Sowwan, M. Local CuO Nanowire Growth on Microhotplates: In Situ Electrical Measurements and Gas Sensing Application. *ACS Sens.* **2016**, *1*, 503–507. [CrossRef]
41. Siegele, M.; Gamauf, C.; Nemecek, A.; Mutinati, G.C.; Steinhauer, S.; Köck, A.; Kraft, J.; Siegert, J.; Schrank, F. Optimized integrated micro-hotplates in CMOS technology. In Proceedings of the IEEE 11th International New Circuits and Systems Conference (NEWCAS), Paris, France, 16–19 June 2013; pp. 1–4. [CrossRef]
42. Steinhauer, S.; Maier, T.; Mutinati, G.C.; Rohracher, K.; Siegert, J.; Schrank, F.; Köck, A. Local synthesis of CuO nanowires on CMOS microhotplates for gas sensing applications. In Proceedings of the TechConnect World Nanotech, Washington, DC, USA, 15–19 June 2014; CRC Press: Boca Raton, FL, USA, 2014; pp. 53–56.

43. Hsu, C.L.; Tsai, J.Y.; Hsueh, T.J. Ethanol gas and humidity sensors of CuO/Cu_2O composite nanowires based on a Cu through-silicon via approach. *Sens. Actuators B Chem.* **2016**, *224*, 95–102. [CrossRef]
44. Alrammouz, R.; Podlecki, J.; Abboud, P.; Sorli, B.; Habchi, R. A review on flexible gas sensors: From materials to devices. *Sens. Actuators A Phys.* **2018**, *284*, 209–231. [CrossRef]
45. Andrysiewicz, W.; Krzeminski, J.; Skarżynski, K.; Marszalek, K.; Sloma, M.; Rydosz, A. Flexible Gas Sensor Printed on a Polymer Substrate for Sub-ppm Acetone Detection. *Electron. Mater. Lett.* **2020**, *16*, 146–155. [CrossRef]
46. Bârsan, N.; Huebner, M.; Weimar, U. Conduction mechanism in semiconducting metal oxide sensing films: impact on transduction. In *Semiconductor Gas Sensors*, 2nd ed.; Jaaniso, R., Tan, O.K., Eds.; Woodhead Publishing Series in Electronic and Optical Materials; Woodhead Publishing: Cambridge, UK, 2020; pp. 39–69. [CrossRef]
47. Ji, H.; Zeng, W.; Li, Y. Gas sensing mechanisms of metal oxide semiconductors: A focus review. *Nanoscale* **2019**, *11*, 22664–22684. [CrossRef] [PubMed]
48. Bejaoui, A.; Guerin, J.; Aguir, K. Modeling of a p-type resistive gas sensor in the presence of a reducing gas. *Sens. Actuators B Chem.* **2013**, *181*, 340–347. [CrossRef]
49. Bejaoui, A.; Guerin, J.; Zapien, J.; Aguir, K. Theoretical and experimental study of the response of CuO gas sensor under ozone. *Sens. Actuators B Chem.* **2014**, *190*, 8–15. [CrossRef]
50. Simion, C.E.; Schipani, F.; Papadogianni, A.; Stanoiu, A.; Budde, M.; Oprea, A.; Weimar, U.; Bierwagen, O.; Barsan, N. Conductance Model for Single-Crystalline/Compact Metal Oxide Gas-Sensing Layers in the Nondegenerate Limit: Example of Epitaxial SnO_2(101). *ACS Sens.* **2019**, *4*, 2420–2428. [CrossRef] [PubMed]
51. Asadzadeh, M.Z.; Köck, A.; Popov, M.; Steinhauer, S.; Spitaler, J.; Romaner, L. Response modeling of single SnO_2 nanowire gas sensors. *Sens. Actuators B Chem.* **2019**, *295*, 22–29. [CrossRef]
52. Hu, J.; Zou, C.; Su, Y.; Li, M.; Han, Y.; Kong, E.S.W.; Yang, Z.; Zhang, Y. An ultrasensitive NO_2 gas sensor based on a hierarchical Cu_2O/CuO mesocrystal nanoflower. *J. Mater. Chem. A* **2018**, *6*, 17120–17131. [CrossRef]
53. Lupan, O.; Ababii, N.; Mishra, A.K.; Gronenberg, O.; Vahl, A.; Schürmann, U.; Duppel, V.; Krüger, H.; Chow, L.; Kienle, L.; et al. Single CuO/Cu_2O/Cu Microwire Covered by a Nanowire Network as a Gas Sensor for the Detection of Battery Hazards. *ACS Appl. Mater. Interfaces* **2020**, *12*, 42248–42263. [CrossRef]
54. Zhang, J.; Liu, M.; Zhang, R.; Wang, B.; Huang, Z. Insight into the properties of stoichiometric, reduced and sulfurized CuO surfaces: Structure sensitivity for H_2S adsorption and dissociation. *Mol. Catal.* **2017**, *438*, 130–142. [CrossRef]
55. Tian, Z.; Bai, H.; Li, Y.; Liu, W.; Li, J.; Kong, Q.; Xi, G. Gas-Sensing Activity of Amorphous Copper Oxide Porous Nanosheets. *ChemistryOpen* **2020**, *9*, 80–86. [CrossRef]
56. Cretu, V.; Postica, V.; Mishra, A.K.; Hoppe, M.; Tiginyanu, I.; Mishra, Y.K.; Chow, L.; de Leeuw, N.H.; Adelung, R.; Lupan, O. Synthesis, characterization and DFT studies of zinc-doped copper oxide nanocrystals for gas sensing applications. *J. Mater. Chem. A* **2016**, *4*, 6527–6539. [CrossRef]
57. Barsan, N.; Koziej, D.; Weimar, U. Metal oxide-based gas sensor research: How to? *Sens. Actuators B Chem.* **2007**, *121*, 18–35. [CrossRef]
58. Tanvir, N.B.; Wilbertz, C.; Steinhauer, S.; Köck, A.; Urban, G.; Yurchenko, O. Work Function Based CO_2 Gas Sensing Using Metal Oxide Nanoparticles at Room Temperature. *Mater. Today Proc.* **2015**, *2*, 4190–4195. [CrossRef]
59. Tanvir, N.B.; Yurchenko, O.; Wilbertz, C.; Urban, G. Investigation of CO_2 reaction with copper oxide nanoparticles for room temperature gas sensing. *J. Mater. Chem. A* **2016**, *4*, 5294–5302. [CrossRef]
60. Tanvir, N.; Yurchenko, O.; Laubender, E.; Urban, G. Investigation of low temperature effects on work function based CO_2 gas sensing of nanoparticulate CuO films. *Sens. Actuators B Chem.* **2017**, *247*, 968–974. [CrossRef]
61. Müller, G.; Prades, J.; Hackner, A.; Ponzoni, A.; Comini, E.; Sberveglieri, G. Sensitivity-Selectivity Trade-Offs in Surface Ionization Gas Detection. *Nanomaterials* **2018**, *8*, 1017. [CrossRef]
62. Wicker, S.; Guiltat, M.; Weimar, U.; Hémeryck, A.; Barsan, N. Ambient Humidity Influence on CO Detection with SnO_2 Gas Sensing Materials. A Combined DRIFTS/DFT Investigation. *J. Phys. Chem. C* **2017**, *121*, 25064–25073. [CrossRef]
63. Degler, D.; Junker, B.; Allmendinger, F.; Weimar, U.; Barsan, N. Investigations on the Temperature-Dependent Interaction of Water Vapor with Tin Dioxide and Its Implications on Gas Sensing. *ACS Sens.* **2020**, *5*, 3207–3216. [CrossRef]
64. Hübner, M.; Simion, C.; Tomescu-Stănoiu, A.; Pokhrel, S.; Bârsan, N.; Weimar, U. Influence of humidity on CO sensing with p-type CuO thick film gas sensors. *Sens. Actuators B Chem.* **2011**, *153*, 347–353. [CrossRef]
65. Steinhauer, S.; Brunet, E.; Maier, T.; Mutinati, G.C.; Köck, A. CuO nanowire gas sensors for CO detection in humid atmosphere. In Proceedings of the Transducers & Eurosensors XXVII, Barcelona, Spain, Barcelona, Spain, 16–20 June 2013. [CrossRef]
66. Miao, J.; Chen, C.; Meng, L.; Lin, Y. Self-Assembled Monolayer of Metal Oxide Nanosheet and Structure and Gas-Sensing Property Relationship. *ACS Sens.* **2019**, *4*, 1279–1290. [CrossRef]
67. Miao, J.; Chen, C.; Lin, J.Y. Humidity independent hydrogen sulfide sensing response achieved with monolayer film of CuO nanosheets. *Sens. Actuators B Chem.* **2020**, *309*, 127785. [CrossRef]
68. Li, D.; Tang, Y.; Ao, D.; Xiang, X.; Wang, S.; Zu, X. Ultra-highly sensitive and selective H_2S gas sensor based on CuO with sub-ppb detection limit. *Int. J. Hydrogen Energy* **2019**, *44*, 3985–3992. [CrossRef]
69. Zhang, F.; Zhu, A.; Luo, Y.; Tian, Y.; Yang, J.; Qin, Y. CuO Nanosheets for Sensitive and Selective Determination of H_2S with High Recovery Ability. *J. Phys. Chem. C* **2010**, *114*, 19214–19219. [CrossRef]

70. Steinhauer, S.; Brunet, E.; Maier, T.; Mutinati, G.; Köck, A. Suspended CuO nanowires for ppb level H_2S sensing in dry and humid atmosphere. *Sens. Actuators B Chem.* **2013**, *186*, 550–556. [CrossRef]
71. Mirzaei, A.; Leonardi, S.; Neri, G. Detection of hazardous volatile organic compounds (VOCs) by metal oxide nanostructures-based gas sensors: A review. *Ceram. Int.* **2016**, *42*, 15119–15141. [CrossRef]
72. Park, H.J.; Choi, N.J.; Kang, H.; Jung, M.Y.; Park, J.W.; Park, K.H.; Lee, D.S. A ppb-level formaldehyde gas sensor based on CuO nanocubes prepared using a polyol process. *Sens. Actuators B Chem.* **2014**, *203*, 282–288. [CrossRef]
73. Deng, H.; Li, H.; Wang, F.; Yuan, C.; Liu, S.; Wang, P.; Xie, L.; Sun, Y.; Chang, F. A high sensitive and low detection limit of formaldehyde gas sensor based on hierarchical flower-like CuO nanostructure fabricated by sol–gel method. *J. Mater. Sci. Mater. Electron.* **2016**, *27*, 6766–6772. [CrossRef]
74. Wang, F.; Li, H.; Yuan, Z.; Sun, Y.; Chang, F.; Deng, H.; Xie, L.; Li, H. A highly sensitive gas sensor based on CuO nanoparticles synthetized via a sol-gel method. *RSC Adv.* **2016**, *6*, 79343–79349. [CrossRef]
75. Lee, J.E.; Kim, D.Y.; Lee, H.K.; Park, H.J.; Ma, A.; Choi, S.Y.; Lee, D.S. Sonochemical synthesis of HKUST-1-based CuO decorated with Pt nanoparticles for formaldehyde gas-sensor applications. *Sens. Actuators B Chem.* **2019**, *292*, 289–296. [CrossRef]
76. Choi, Y.M.; Cho, S.Y.; Jang, D.; Koh, H.J.; Choi, J.; Kim, C.H.; Jung, H.T. Ultrasensitive Detection of VOCs Using a High-Resolution CuO/Cu_2O/Ag Nanopattern Sensor. *Adv. Funct. Mater.* **2019**, *29*, 1808319. [CrossRef]
77. Szkudlarek, A.; Kollbek, K.; Klejna, S.; Rydosz, A. Electronic sensitization of CuO thin films by Cr-doping for enhanced gas sensor response at low detection limit. *Mater. Res. Express* **2018**, *5*, 126406. [CrossRef]
78. Xia, S.; Zhu, H.; Cai, H.; Zhang, J.; Yu, J.; Tang, Z. Hydrothermally synthesized CuO based volatile organic compound gas sensor. *RSC Adv.* **2014**, *4*, 57975–57982. [CrossRef]
79. Dong, C.; Xing, X.; Chen, N.; Liu, X.; Wang, Y. Biomorphic synthesis of hollow CuO fibers for low-ppm-level n-propanol detection via a facile solution combustion method. *Sens. Actuators B Chem.* **2016**, *230*, 1–8. [CrossRef]
80. Wang, T.; Xiao, Q. Solvothermal synthesis and sensing properties of meso-macroporous hierarchical CuO microspheres composed of nanosheets. *Mater. Chem. Phys.* **2013**, *139*, 603–608. [CrossRef]
81. Yang, B.; Liu, J.; Qin, H.; Liu, Q.; Jing, X.; Zhang, H.; Li, R.; Huang, G.; Wang, J. PtO_2-nanoparticles functionalized CuO polyhedrons for n-butanol gas sensor application. *Ceram. Int.* **2018**, *44*, 10426–10432. [CrossRef]
82. Tan, J.; Dun, M.; Li, L.; Zhao, J.; Li, X.; Hu, Y.; Huang, G.; Tan, W.; Huang, X. Self-template derived CuO nanowires assembled microspheres and its gas sensing properties. *Sens. Actuators B Chem.* **2017**, *252*, 1–8. [CrossRef]
83. Hien, V.X.; Minh, N.H.; Son, D.T.; Nghi, N.T.; Phuoc, L.H.; Khoa, C.T.; Vuong, D.D.; Chien, N.D.; Heo, Y.W. Acetone sensing properties of CuO nanowalls synthesized via oxidation of Cu foil in aqueous NH4OH. *Vacuum* **2018**, *150*, 129–135. [CrossRef]
84. Liu, X.; Zhang, J.; Kang, Y.; Wu, S.; Wang, S. Brochantite tabular microspindles and their conversion to wormlike CuO structures for gas sensing. *CrystEngComm* **2012**, *14*, 620–625. [CrossRef]
85. Mazhar, M.; Faglia, G.; Comini, E.; Zappa, D.; Baratto, C.; Sberveglieri, G. Kelvin probe as an effective tool to develop sensitive p-type CuO gas sensors. *Sens. Actuators B Chem.* **2016**, *222*, 1257–1263. [CrossRef]
86. Mnethu, O.; Nkosi, S.S.; Kortidis, I.; Motaung, D.E.; Kroon, R.; Swart, H.C.; Ntsasa, N.G.; Tshilongo, J.; Moyo, T. Ultra-sensitive and selective p-xylene gas sensor at low operating temperature utilizing Zn doped CuO nanoplatelets: Insignificant vestiges of oxygen vacancies. *J. Colloid Interface Sci.* **2020**, *576*, 364–375. [CrossRef]
87. Lupan, O.; Postica, V.; Cretu, V.; Wolff, N.; Duppel, V.; Kienle, L.; Adelung, R. Single and networked CuO nanowires for highly sensitive p-type semiconductor gas sensor applications. *Phys. Status Solidi RRL Rapid Res. Lett.* **2016**, *10*, 260–266. [CrossRef]
88. Gou, X.; Wang, G.; Yang, J.; Park, J.; Wexler, D. Chemical synthesis, characterisation and gas sensing performance of copper oxide nanoribbons. *J. Mater. Chem.* **2008**, *18*, 965–969. [CrossRef]
89. Taubert, A.; Stange, F.; Li, Z.; Junginger, M.; Günter, C.; Neumann, M.; Friedrich, A. CuO Nanoparticles from the Strongly Hydrated Ionic Liquid Precursor (ILP) Tetrabutylammonium Hydroxide: Evaluation of the Ethanol Sensing Activity. *ACS Appl. Mater. Interfaces* **2012**, *4*, 791–795. [CrossRef] [PubMed]
90. Wang, L.; Zhang, R.; Zhou, T.; Lou, Z.; Deng, J.; Zhang, T. Concave Cu_2O octahedral nanoparticles as an advanced sensing material for benzene (C_6H_6) and nitrogen dioxide (NO_2) detection. *Sens. Actuators B Chem.* **2016**, *223*, 311–317. [CrossRef]
91. Wu, Y.P.; Zhou, W.; Dong, W.W.; Zhao, J.; Qiao, X.Q.; Hou, D.F.; Li, D.S.; Zhang, Q.; Feng, P. Temperature-Controlled Synthesis of Porous CuO Particles with Different Morphologies for Highly Sensitive Detection of Triethylamine. *Cryst. Growth Des.* **2017**, *17*, 2158–2165. [CrossRef]
92. Sui, Y.; Zeng, Y.; Zheng, W.; Liu, B.; Zou, B.; Yang, H. Synthesis of polyhedron hollow structure Cu_2O and their gas-sensing properties. *Sens. Actuators B Chem.* **2012**, *171–172*, 135–140. [CrossRef]
93. Sui, Y.; Zeng, Y.; Fu, L.; Zheng, W.; Li, D.; Liu, B.; Zou, B. Low-temperature synthesis of porous hollow structured Cu_2O for photocatalytic activity and gas sensor application. *RSC Adv.* **2013**, *3*, 18651–18660. [CrossRef]
94. Zhang, H.; Zhu, Q.; Zhang, Y.; Wang, Y.; Zhao, L.; Yu, B. One-Pot Synthesis and Hierarchical Assembly of Hollow Cu_2O Microspheres with Nanocrystals-Composed Porous Multishell and Their Gas-Sensing Properties. *Adv. Funct. Mater.* **2007**, *17*, 2766–2771. [CrossRef]
95. Oosthuizen, D.; Korditis, I.; Swart, H.; Motaung, D. Facile control of room temperature nitrogen dioxide gas selectivity induced by copper oxide nanoplatelets. *J. Colloid Interface Sci.* **2020**, *560*, 755–768. [CrossRef]
96. Umar, A.; Alshahrani, A.; Algarni, H.; Kumar, R. CuO nanosheets as potential scaffolds for gas sensing applications. *Sens. Actuators B Chem.* **2017**, *250*, 24–31. [CrossRef]

97. Zhang, H.; Li, H.; Cai, L.; Lei, Q.; Wang, J.; Fan, W.; Shi, K.; Han, G. Performances of In-doped CuO-based heterojunction gas sensor. *J. Mater. Sci. Mater. Electron.* **2020**, *31*, 910–919. [CrossRef]
98. Zhou, S.; Chen, M.; Lu, Q.; Hu, J.; Wang, H.; Li, K.; Li, K.; Zhang, J.; Zhu, Z.; Liu, Q. Design of hollow dodecahedral Cu_2O nanocages for ethanol gas sensing. *Mater. Lett.* **2019**, *247*, 15–18. [CrossRef]
99. Zhang, J.; Liu, J.; Peng, Q.; Wang, X.; Li, Y. Nearly Monodisperse Cu_2O and CuO Nanospheres: Preparation and Applications for Sensitive Gas Sensors. *Chem. Mater.* **2006**, *18*, 867–871. [CrossRef]
100. Yang, C.; Xiao, F.; Wang, J.; Su, X. 3D flower- and 2D sheet-like CuO nanostructures: Microwave-assisted synthesis and application in gas sensors. *Sens. Actuators B Chem.* **2015**, *207*, 177–185. [CrossRef]
101. Yan, H.; Tian, X.; Sun, J.; Ma, F. Enhanced sensing properties of CuO nanosheets for volatile organic compounds detection. *J. Mater. Sci. Mater. Electron.* **2015**, *26*, 280–287. [CrossRef]
102. Yan, H.; Tian, X.; Ma, F.; Sun, J. CuO nanoparticles fabricated by direct thermo-oxidation of sputtered Cu film for VOCs detection. *Sens. Actuators B Chem.* **2015**, *221*, 599–605. [CrossRef]
103. Hsueh, H.T.; Chang, S.J.; Hung, F.Y.; Weng, W.Y.; Hsu, C.L.; Hsueh, T.J.; Lin, S.S.; Dai, B.T. Ethanol Gas Sensor of Crabwise CuO Nanowires Prepared on Glass Substrate. *J. Electrochem. Soc.* **2011**, *158*, J106. [CrossRef]
104. Li, T.; He, M.; Zeng, W. Polyhedral Cu_2O crystal: Morphology evolution from meshed nanocube to solid and gas-sensing performance. *J. Alloys Compd.* **2017**, *712*, 50–58. [CrossRef]
105. Ghosh, A.; Maity, A.; Banerjee, R.; Majumder, S. Volatile organic compound sensing using copper oxide thin films: Addressing the cross sensitivity issue. *J. Alloys Compd.* **2017**, *692*, 108–118. [CrossRef]
106. Zhou, L.J.; Zou, Y.C.; Zhao, J.; Wang, P.P.; Feng, L.L.; Sun, L.W.; Wang, D.J.; Li, G.D. Facile synthesis of highly stable and porous Cu_2O/CuO cubes with enhanced gas sensing properties. *Sens. Actuators B Chem.* **2013**, *188*, 533–539. [CrossRef]
107. Choi, Y.H.; Kim, D.H.; Han, H.S.; Shin, S.; Hong, S.H.; Hong, K.S. Direct Printing Synthesis of Self-Organized Copper Oxide Hollow Spheres on a Substrate Using Copper(II) Complex Ink: Gas Sensing and Photoelectrochemical Properties. *Langmuir* **2014**, *30*, 700–709. [CrossRef]
108. Choi, Y.H.; Kim, D.H.; Hong, S.H.; Hong, K.S. H_2 and C_2H_5OH sensing characteristics of mesoporous p-type CuO films prepared via a novel precursor-based ink solution route. *Sens. Actuators B Chem.* **2013**, *178*, 395–403. [CrossRef]
109. Mirzaei, A.; Kim, S.S.; Kim, H.W. Resistance-based H_2S gas sensors using metal oxide nanostructures: A review of recent advances. *J. Hazard. Mater.* **2018**, *357*, 314–331. [CrossRef]
110. Steinhauer, S. Gas Sensing Properties of Metal Oxide Nanowires and Their CMOS Integration. Ph.D. Thesis, TU Wien, Vienna, Austria, 2014.
111. Henzler, K.; Heilemann, A.; Kneer, J.; Guttmann, P.; Jia, H.; Bartsch, E.; Lu, Y.; Palzer, S. Investigation of reactions between trace gases and functional CuO nanospheres and octahedrons using NEXAFS-TXM imaging. *Sci. Rep.* **2015**, *5*, 17729. [CrossRef] [PubMed]
112. Kneer, J.; Wöllenstein, J.; Palzer, S. Specific, trace gas induced phase transition in copper(II)oxide for highly selective gas sensing. *Appl. Phys. Lett.* **2014**, *105*, 073509. [CrossRef]
113. Hennemann, J.; Kohl, C.D.; Smarsly, B.M.; Metelmann, H.; Rohnke, M.; Janek, J.; Reppin, D.; Meyer, B.K.; Russ, S.; Wagner, T. Copper oxide based H_2S dosimeters—Modeling of percolation and diffusion processes. *Sens. Actuators B Chem.* **2015**, *217*, 41–50. [CrossRef]
114. Hennemann, J.; Kohl, C.D.; Smarsly, B.M.; Sauerwald, T.; Teissier, J.M.; Russ, S.; Wagner, T. CuO thin films for the detection of H_2S doses: Investigation and application. *Phys. Status Solidi A* **2015**, *212*, 1281–1288. [CrossRef]
115. Kneer, J.; Knobelspies, S.; Bierer, B.; Wöllenstein, J.; Palzer, S. New method to selectively determine hydrogen sulfide concentrations using CuO layers. *Sens. Actuators B Chem.* **2016**, *222*, 625–631. [CrossRef]
116. Su, Y.; Li, G.; Guo, Z.; Li, Y.Y.; Li, Y.X.; Huang, X.J.; Liu, J.H. Cation-Exchange Synthesis of Cu_2Se Nanobelts and Thermal Conversion to Porous CuO Nanobelts with Highly Selective Sensing toward H_2S. *ACS Appl. Nano Mater.* **2018**, *1*, 245–253. [CrossRef]
117. Li, Z.; Wang, N.; Lin, Z.; Wang, J.; Liu, W.; Sun, K.; Fu, Y.Q.; Wang, Z. Room-Temperature High-Performance H_2S Sensor Based on Porous CuO Nanosheets Prepared by Hydrothermal Method. *ACS Appl. Mater. Interfaces* **2016**, *8*, 20962–20968. [CrossRef] [PubMed]
118. Li, X.; Wang, Y.; Lei, Y.; Gu, Z. Highly sensitive H_2S sensor based on template-synthesized CuO nanowires. *RSC Adv.* **2012**, *2*, 2302–2307. [CrossRef]
119. Qin, Y.; Zhang, F.; Chen, Y.; Zhou, Y.; Li, J.; Zhu, A.; Luo, Y.; Tian, Y.; Yang, J. Hierarchically Porous CuO Hollow Spheres Fabricated via a One-Pot Template-Free Method for High-Performance Gas Sensors. *J. Phys. Chem. C* **2012**, *116*, 11994–12000. [CrossRef]
120. Meng, F.N.; Di, X.P.; Dong, H.W.; Zhang, Y.; Zhu, C.L.; Li, C.; Chen, Y.J. Ppb H_2S gas sensing characteristics of Cu_2O/CuO sub-microspheres at low-temperature. *Sens. Actuators B Chem.* **2013**, *182*, 197–204. [CrossRef]
121. Wu, K.; Zhang, C. Facile synthesis and ppb-level H_2S sensing performance of hierarchical CuO microflowers assembled with nano-spindles. *J. Mater. Sci. Mater. Electron.* **2020**, *31*, 7937–7945. [CrossRef]
122. Park, S.; Cai, Z.; Lee, J.; Yoon, J.; Chang, S.P. Fabrication of a low-concentration H_2S gas sensor using CuO nanorods decorated with Fe_2O_3 nanoparticles. *Mater. Lett.* **2016**, *181*, 231–235. [CrossRef]
123. Ramgir, N.; Ganapathi, S.K.; Kaur, M.; Datta, N.; Muthe, K.; Aswal, D.; Gupta, S.; Yakhmi, J. Sub-ppm H_2S sensing at room temperature using CuO thin films. *Sens. Actuators B Chem.* **2010**, *151*, 90–96. [CrossRef]

124. Chen, Y.J.; Meng, F.N.; Yu, H.L.; Zhu, C.L.; Wang, T.S.; Gao, P.; ; Ouyang, ; Y. Sonochemical synthesis and ppb H_2S sensing performances of CuO nanobelts. *Sens. Actuators B Chem.* **2013**, *176*, 15–21. [CrossRef]
125. Tang, Q.; Hu, X.B.; He, M.; Xie, L.L.; Zhu, Z.G.; Wu, J.Q. Effect of Platinum Doping on the Morphology and Sensing Performance for CuO-Based Gas Sensor. *Appl. Sci.* **2018**, *8*, 1091. [CrossRef]
126. Li, Z.; Wang, J.; Wang, N.; Yan, S.; Liu, W.; Fu, Y.Q.; Wang, Z. Hydrothermal synthesis of hierarchically flower-like CuO nanostructures with porous nanosheets for excellent H_2S sensing. *J. Alloys Compd.* **2017**, *725*, 1136–1143. [CrossRef]
127. Hu, X.; Zhu, Z.; Chen, C.; Wen, T.; Zhao, X.; Xie, L. Highly sensitive H_2S gas sensors based on Pd-doped CuO nanoflowers with low operating temperature. *Sens. Actuators B Chem.* **2017**, *253*, 809–817. [CrossRef]
128. Xu, Z.; Luo, Y.; Duan, G. Self-Assembly of Cu_2O Monolayer Colloidal Particle Film Allows the Fabrication of CuO Sensor with Superselectivity for Hydrogen Sulfide. *ACS Appl. Mater. Interfaces* **2019**, *11*, 8164–8174. [CrossRef]
129. Van Tong, P.; Hoa, N.D.; Nha, H.T.; Van Duy, N.; Hung, C.M.; Van Hieu, N. SO_2 and H_2S Sensing Properties of Hydrothermally Synthesized CuO Nanoplates. *J. Electron. Mater.* **2018**, *47*, 7170–7178. [CrossRef]
130. Kim, J.H.; Mirzaei, A.; Zheng, Y.; Lee, J.H.; Kim, J.Y.; Kim, H.W.; Kim, S.S. Enhancement of H_2S sensing performance of p-CuO nanofibers by loading p-reduced graphene oxide nanosheets. *Sens. Actuators B Chem.* **2019**, *281*, 453–461. [CrossRef]
131. Zhou, J.; Ikram, M.; Rehman, A.U.; Wang, J.; Zhao, Y.; Kan, K.; Zhang, W.; Raziq, F.; Li, L.; Shi, K. Highly selective detection of NH_3 and H_2S using the pristine CuO and mesoporous In_2O_3@CuO multijunctions nanofibers at room temperature. *Sens. Actuators B Chem.* **2018**, *255*, 1819–1830. [CrossRef]
132. Ding, J.; Wang, D.; Wang, X.; Wang, X.; Tian, L.; Zhang, Y.; Chai, Z.; Hu, Q. Tailoring responsivity with engineered porous Cu_2O hexapods architecture towards high-performance H_2S gas-sensing. *J. Mater. Sci. Mater. Electron.* **2019**, *30*, 16627–16635. [CrossRef]
133. Kim, H.; Jin, C.; Park, S.; Kim, S.; Lee, C. H_2S gas sensing properties of bare and Pd-functionalized CuO nanorods. *Sens. Actuators B Chem.* **2012**, *161*, 594–599. [CrossRef]
134. Mahajan, S.; Jagtap, S. Metal-oxide semiconductors for carbon monoxide (CO) gas sensing: A review. *Appl. Mater. Today* **2020**, *18*, 100483. [CrossRef]
135. Choi, S.W.; Park, J.Y.; Kim, S.S. Growth behavior and sensing properties of nanograins in CuO nanofibers. *Chem. Eng. J.* **2011**, *172*, 550–556. [CrossRef]
136. Ambardekar, V.; Bandyopadhyay, P.; Majumder, S. Plasma sprayed copper oxide sensor for selective sensing of carbon monoxide. *Mater. Chem. Phys.* **2021**, *258*, 123966. [CrossRef]
137. Liao, L.; Zhang, Z.; Yan, B.; Zheng, Z.; Bao, Q.L.; Wu, T.; Li, C.M.; Shen, Z.X.; Zhang, J.X.; Gong, H.; et al. Multifunctional CuO nanowire devices: p-type field effect transistors and CO gas sensors. *Nanotechnology* **2009**, *20*, 085203. [CrossRef] [PubMed]
138. Oosthuizen, D.; Motaung, D.; Swart, H. Selective detection of CO at room temperature with CuO nanoplatelets sensor for indoor air quality monitoring manifested by crystallinity. *Appl. Surf. Sci.* **2019**, *466*, 545–553. [CrossRef]
139. Kim, Y.S.; Hwang, I.S.; Kim, S.J.; Lee, C.Y.; Lee, J.H. CuO nanowire gas sensors for air quality control in automotive cabin. *Sens. Actuators B Chem.* **2008**, *135*, 298–303. [CrossRef]
140. Liu, Q.; Cui, Z.; Zhang, Q.; Guo, L. Gold-catalytic green synthesis of Cu_2O/Au/CuO hierarchical nanostructure and application for CO gas sensor. *Chin. Sci. Bull.* **2014**, *59*, 7–10. [CrossRef]
141. Molavi, R.; Sheikhi, M. Facile wet chemical synthesis of Al doped CuO nanoleaves for carbon monoxide gas sensor applications. *Mater. Sci. Semicond. Process.* **2020**, *106*, 104767. [CrossRef]
142. Köck, A.; Chitu, L.; Defregger, S.; Kraker, E.; Maier, G.; Steinhauer, S.; Wimmer-Teubenbacher, R. Metal Oxide Nanowires for Gas Sensor Applications. *BHM Berg-und Hüttenmännische Monatshefte* **2014**, *159*, 385–389. [CrossRef]
143. Steinhauer, S.; Singh, V.; Cassidy, C.; Gspan, C.; Grogger, W.; Sowwan, M.; Köck, A. Single CuO nanowires decorated with size-selected Pd nanoparticles for CO sensing in humid atmosphere. *Nanotechnology* **2015**, *26*, 175502. [CrossRef]
144. Zou, C.; Wang, J.; Liang, F.; Xie, W.; Shao, L.; Fu, D. Large-area aligned CuO nanowires arrays: Synthesis, anomalous ferromagnetic and CO gas sensing properties. *Curr. Appl. Phys.* **2012**, *12*, 1349–1354. [CrossRef]
145. Aslani, A.; Oroojpour, V. CO gas sensing of CuO nanostructures, synthesized by an assisted solvothermal wet chemical route. *Phys. B Condens. Matter* **2011**, *406*, 144–149. [CrossRef]
146. Mulmi, S.; Thangadurai, V. Editors' Choice—Review—Solid-State Electrochemical Carbon Dioxide Sensors: Fundamentals, Materials and Applications. *J. Electrochem. Soc.* **2020**, *167*, 037567. [CrossRef]
147. Joshi, S.; Ippolito, S.J.; Periasamy, S.; Sabri, Y.M.; Sunkara, M.V. Efficient Heterostructures of Ag@CuO/$BaTiO_3$ for Low-Temperature CO_2 Gas Detection: Assessing the Role of Nanointerfaces during Sensing by Operando DRIFTS Technique. *ACS Appl. Mater. Interfaces* **2017**, *9*, 27014–27026. [CrossRef] [PubMed]
148. Chapelle, A.; Barnabé, A.; Presmanes, L.; Tailhades, P. Copper and iron based thin film nanocomposites prepared by radio-frequency sputtering. Part II: Elaboration and characterization of oxide/oxide thin film nanocomposites using controlled ex-situ oxidation process. *J. Mater. Sci.* **2013**, *48*, 3304–3314. [CrossRef]
149. Tanvir, N.; Yurchenko, O.; Laubender, E.; Pohle, R.; Sicard, O.; Urban, G. Zinc peroxide combustion promoter in preparation of CuO layers for conductometric CO_2 sensing. *Sens. Actuators B Chem.* **2018**, *257*, 1027–1034. [CrossRef]
150. Wimmer-Teubenbacher, R.; Sosada-Ludwikowska, F.; Zaragoza Travieso, B.; Defregger, S.; Tokmak, O.; Niehaus, J.; Deluca, M.; Köck, A. CuO Thin Films Functionalized with Gold Nanoparticles for Conductometric Carbon Dioxide Gas Sensing. *Chemosensors* **2018**, *6*, 56. [CrossRef]

151. Schieweck, A.; Uhde, E.; Salthammer, T.; Salthammer, L.C.; Morawska, L.; Mazaheri, M.; Kumar, P. Smart homes and the control of indoor air quality. *Renew. Sustain. Energy Rev.* **2018**, *94*, 705–718. [CrossRef]
152. Sohail, M.; Sun, D.W.; Zhu, Z. Recent developments in intelligent packaging for enhancing food quality and safety. *Crit. Rev. Food Sci. Nutr.* **2018**, *58*, 2650–2662. [CrossRef]
153. Sharma, B.; Sharma, A.; Kim, J.S. Recent advances on H_2 sensor technologies based on MOX and FET devices: A review. *Sens. Actuators B Chem.* **2018**, *262*, 758–770. [CrossRef]
154. Lupan, O.; Postica, V.; Ababii, N.; Hoppe, M.; Cretu, V.; Tiginyanu, I.; Sontea, V.; Pauporté, T.; Viana, B.; Adelung, R. Influence of CuO nanostructures morphology on hydrogen gas sensing performances. *Microelectron. Eng.* **2016**, *164*, 63–70. [CrossRef]
155. Kumar, S.; Pavelyev, V.; Mishra, P.; Tripathi, N.; Sharma, P.; Calle, F. A review on 2D transition metal di-chalcogenides and metal oxide nanostructures based NO_2 gas sensors. *Mater. Sci. Semicond. Process.* **2020**, *107*, 104865. [CrossRef]
156. Kneer, J.; Wöllenstein, J.; Palzer, S. Manipulating the gas–surface interaction between copper(II) oxide and mono-nitrogen oxides using temperature. *Sens. Actuators B Chem.* **2016**, *229*, 57–62. [CrossRef]
157. Wang, W.; Zhang, Y.; Zhang, J.; Li, G.; Leng, D.; Gao, Y.; Gao, J.; Lu, H.; Li, X. Metal–organic framework-derived Cu_2O–CuO octahedrons for sensitive and selective detection of ppb-level NO_2 at room temperature. *Sens. Actuators B Chem.* **2021**, *328*, 129045. [CrossRef]
158. Kim, J.Y.; Cho, S.Y.; Jung, H.T. Selective Functionalization of High-Resolution Cu_2O Nanopatterns via Galvanic Replacement for Highly Enhanced Gas Sensing Performance. *Sensors* **2018**, *18*, 4438. [CrossRef]
159. Jia, H.; Gao, H.; Mei, S.; Kneer, J.; Lin, X.; Ran, Q.; Wang, F.; Palzer, S.; Lu, Y. Cu_2O@PNIPAM core–shell microgels as novel inkjet materials for the preparation of CuO hollow porous nanocubes gas sensing layers. *J. Mater. Chem. C* **2018**, *6*, 7249–7256. [CrossRef]
160. Navale, Y.; Navale, S.; Galluzzi, M.; Stadler, F.; Debnath, A.; Ramgir, N.; Gadkari, S.; Gupta, S.; Aswal, D.; Patil, V. Rapid synthesis strategy of CuO nanocubes for sensitive and selective detection of NO_2. *J. Alloys Compd.* **2017**, *708*, 456–463. [CrossRef]
161. Rzaij, J.M.; Habubi, N.F. Room temperature gas sensor based on La_2O_3 doped CuO thin films. *Appl. Phys. A* **2020**, *126*, 560. [CrossRef]
162. Das, A.; Venkataramana, B.; Partheephan, D.; Prasad, A.; Dhara, S.; Tyagi, A. Facile synthesis of nanostructured CuO for low temperature NO_2 sensing. *Phys. E Low Dimens. Syst. Nanostruct.* **2013**, *54*, 40–44. [CrossRef]
163. Kim, K.M.; Jeong, H.M.; Kim, H.R.; Choi, K.I.; Kim, H.J.; Lee, J.H. Selective Detection of NO_2 Using Cr-Doped CuO Nanorods. *Sensors* **2012**, *12*, 8013–8025. [CrossRef]
164. Zappa, D.; Comini, E.; Zamani, R.; Arbiol, J.; Morante, J.; Sberveglieri, G. Preparation of copper oxide nanowire-based conductometric chemical sensors. *Sens. Actuators B Chem.* **2013**, *182*, 7–15. [CrossRef]
165. Hansen, B.J.; Kouklin, N.; Lu, G.; Lin, I.K.; Chen, J.; Zhang, X. Transport, Analyte Detection, and Opto-Electronic Response of p-Type CuO Nanowires. *J. Phys. Chem. C* **2010**, *114*, 2440–2447. [CrossRef]
166. Bhuvaneshwari, S.; Gopalakrishnan, N. Enhanced ammonia sensing characteristics of Cr doped CuO nanoboats. *J. Alloys Compd.* **2016**, *654*, 202–208. [CrossRef]
167. Mashock, M.; Yu, K.; Cui, S.; Mao, S.; Lu, G.; Chen, J. Modulating Gas Sensing Properties of CuO Nanowires through Creation of Discrete Nanosized p–n Junctions on Their Surfaces. *ACS Appl. Mater. Interfaces* **2012**, *4*, 4192–4199. [CrossRef] [PubMed]
168. Jayatissa, A.H.; Samarasekara, P.; Kun, G. Methane gas sensor application of cuprous oxide synthesized by thermal oxidation. *Phys. Status Solidi A* **2009**, *206*, 332–337. [CrossRef]
169. Feng, S.; Farha, F.; Li, Q.; Wan, Y.; Xu, Y.; Zhang, T.; Ning, H. Review on Smart Gas Sensing Technology. *Sensors* **2019**, *19*, 3760. [CrossRef]
170. Shi, Q.; Dong, B.; He, T.; Sun, Z.; Zhu, J.; Zhang, Z.; Lee, C. Progress in wearable electronics/photonics—Moving toward the era of artificial intelligence and internet of things. *InfoMat* **2020**, *2*, 1131–1162. [CrossRef]
171. Steinhauer, S.; Wang, Z.; Zhou, Z.; Krainer, J.; Köck, A.; Nordlund, K.; Djurabekova, F.; Grammatikopoulos, P.; Sowwan, M. Probing electron beam effects with chemoresistive nanosensors during in situ environmental transmission electron microscopy. *Appl. Phys. Lett.* **2017**, *110*, 094103. [CrossRef]
172. Steinhauer, S.; Vernieres, J.; Krainer, J.; Köck, A.; Grammatikopoulos, P.; Sowwan, M. In situ chemoresistive sensing in the environmental TEM: probing functional devices and their nanoscale morphology. *Nanoscale* **2017**, *9*, 7380–7384. [CrossRef] [PubMed]
173. Volanti, D.P.; Felix, A.A.; Suman, P.H.; Longo, E.; Varela, J.A.; Orlandi, M.O. Monitoring a CuO gas sensor at work: an advanced in situ X-ray absorption spectroscopy study. *Phys. Chem. Chem. Phys.* **2015**, *17*, 18761–18767. [CrossRef] [PubMed]
174. Hozák, P.; Vorokhta, M.; Khalakhan, I.; Jarkovská, K.; Cibulková, J.; Fitl, P.; Vlček, J.; Fara, J.; Tomeček, D.; Novotný, M.; et al. New Insight into the Gas-Sensing Properties of CuO_x Nanowires by Near-Ambient Pressure XPS. *J. Phys. Chem. C* **2019**, *123*, 29739–29749. [CrossRef]